Convolutional neural networks to predict the onset of oscillatory instabilities in turbulent systems

Eustaquio A. Ruiz, Vishnu R. Unni, A. Induja Pavithran, R. I. Sujith, and Abhishek Saha $^{1,\,b}$

¹⁾Dept. Mechanical and Aerospace Engineering, University of California San Diego, La Jolla, CA 92093, USA

²⁾Dept. Aerospace Engineering, Indian Institute of Technology Madras, Madras, TN 600036, India

(Dated: 1 May 2025)

Many fluid dynamic systems exhibit undesirable oscillatory instabilities due to positive feedback between fluctuations in their different subsystems. Thermoacoustic instability, aeroacoustic instability, and aeroelastic instability are some examples. When the fluid flow in the system is turbulent, the approach to such oscillatory instabilities occurs through a universal route characterized by a dynamical regime known as intermittency. In this manuscript, we extract the peculiar pattern of phase space attractors during the regime of intermittency by constructing recurrence networks corresponding to the phase space topology. We further train a convolutional neural network to classify the periodic and aperiodic structures in the recurrence networks and define a measure that indicates the proximity of the dynamical state to the onset of oscillatory instability. We show that this measure can predict the onset of oscillatory instability in three different fluid dynamic systems governed by different physical phenomena.

Keywords: Convolution Neural Network, Recurrence Network, Flow instability

a) Electronic mail: Email: vishnu.runni@gmail.com

b) Electronic mail: Email: asaha@eng.ucsd.edu

Practical dynamical systems often exhibit very complex phase space dynamics, and their phase space topology is constituted by interwoven salient features (patterns). The relative strength of these salient features that determine the dynamical state of the system, when quantified, can be used to track the evolution of the state of the system, anticipate critical transitions in the system, and even introduce effective control of the system. In the current study, a methodology to analyze and quantify complex patterns in the phase space of a dynamical system using convolutional neural networks (CNN) has been developed. The methodology classifies salient features in the phase space of a system by analyzing patterns (feature detection) in the corresponding recurrence network using CNN. We then use this methodology to predict the onset of oscillatory instability in fluid dynamic systems, namely, thermoacoustic instability, aeroacoustic instability, and aeroelastic instability. A priory prediction of such oscillatory instability is beneficial since they are often highly disastrous.

I. INTRODUCTION

Oscillatory instabilities resulting from the feedback between the flow and other subsystems are common in many fluid dynamical systems. For example, when combustion occurs inside a confinement, as is the case for many practical systems, the unsteadiness in the heat release rate often gets mutually coupled with the acoustic field of the confinement. When there is a positive feedback between them, a growth of amplitude of pressure fluctuations is observed. As pressure fluctuations grow, the nonlinearities cause the saturation of the amplitude, eventually leading to sustained large amplitude periodic oscillations - a phenomenon known as thermoacoustic instability. Combustors in rocket engines and gas turbines are susceptible to such instability which, in turn, cause catastrophic hardware damages^{1,2}.

Aeroacoustic instability is another such oscillatory instability. A fluid flow past obstructions, over a cavity, or separating from a boundary, produces pressure perturbations due to unsteady phenomena such as vorticity fluctuations, shear layer oscillations, and turbulence^{3,4}. When these perturbations get coupled with the acoustic field of the system establishing a positive feedback, the acoustic oscillations in the system can grow and saturate

into strong periodic oscillations. While such aeroacoustic instabilities could be pleasant and harmless as in the case of sounds produced by wind instruments or bird songs, they also cause unwanted phenomena such as screech in jets with shocks⁵ and howling of ejectors⁶. There are several reviews that detail various studies on aeroacoustic instability^{7–9}.

Oscillatory instabilities are also common in structural elements suspended in fluid flows. Commonly known as aeroelastic instabilities, these instabilities are the result of a positive coupling among the elastic, inertial, and aerodynamic forces. These undesired and potentially catastrophic sustained oscillations of the structure are also known as aeroelastic flutter. Such instabilities affect elastic bodies such as airplanes, wind turbines, skyscrapers, and suspension bridges. A famous example of destruction caused by aeroelastic instability is the collapse of the Tacoma Narrow bridge¹⁰. Although these instabilities and associated dynamics have been studied over a long time, prognosis and mitigation of these oscillations remain a serious challenge^{1,2,7,11}.

Nonlinearities associated with the fluid dynamic system, in many scenarios, make it difficult to predict the onset of such oscillatory instabilities. Nevertheless, there have been substantial number of studies focused on developing precursors to such instabilities in different systems. Traditional methodologies rely on tracking the temporal variations in root mean square of time series of one or more state variables of the system (e.g., pressure or strain fluctuations), studying the evolution of peaks in Fourier transformation/ wavelet transformation of time-series of state variables, etc^{12,13}. While these measures could indicate an onset of oscillatory instability, in most cases the warning time they provide is inadequate for any meaningful control action, making them unreliable precursors.

Recent studies indicate that when the underlying flow is turbulent, the transition regime from safe operation to oscillatory instability is characterized by a dynamical state of intermittency during which the system exhibits bursts of large amplitude periodic oscillations amidst low amplitude aperiodic fluctuations^{14–19}. As fluid dynamic systems approach oscillatory instability, the duration for which the large amplitude periodic bursts persist during the intermittent oscillations progressively increase. This discovery of gradual morphing of intermittency to periodicity during the emergence oscillatory instability set-off a new wave of investigations into precursory signals focused on quantifying the intermittency statistics²⁰.

The presence of the dynamical state of intermittency in the transition regime to oscillatory instability was first identified in aeroelastic systems by Korbahti et al.¹⁴. Parallelly,

Nair et al. identified intermittency prior to the inception of thermoacoustic instability²¹ and aeroacoustic instability¹⁶. Recent works have been focused on quantifying various intermittency statistics using nonlinear statistical methods such as multifractal analysis²², symbolic time series analysis²³, recurrence quantification^{21,24} and topological characterization of complex networks^{25,26}, in order to use such statistics as early warning measures for impending oscillatory instability. Very recently, Pavithran et al.¹⁸ showed that in turbulent systems there exists a universal pattern indicated by a universal scaling behavior between the fractal dimension of the time series of the unsteady state variable, and the amplitude for the dominant frequency in its amplitude spectrum. Pavithran et al.¹⁹ later also showed that the spectral condensation associated with the onset of oscillatory instability exhibits a universal behavior.

In this paper, we aim to detect and quantify this universal pattern during the emergence of oscillatory instability in fluid dynamic systems, and use them for prognosis. Towards this, we propose a method to estimate relative dominance of salient features, constituting the phase space of a practical system, by characterizing the patterns in the recurrence networks (RN) corresponding to state variables of the system. Furthermore, we will use Convolutional Neural Networks (CNN), a popular machine learning tool to achieve such goal. Recurrence analysis is a dynamical systems approach to study how the trajectory of state points corresponding to a system revisits the same part of the phase space in time. It helps us represent the complex topology of a multidimensional phase space attractor in a two dimensional space. The inherently nonlinear time series analysis method of recurrence quantification was previously used by Nair et al.^{21,27}, and Gotoda et al.²⁴ to develop precursors for the onset thermoacoustic instability. Godavarthi et al.²⁸ used recurrence network analysis to study the synchronization and causal relationship between pressure and heat release fluctuations in a turbulent combustor.

While the above studies used statistical measures that quantify the patterns in the recurrence plots, the present study will use the power of deep learning to detect hidden patterns in recurrence plots elusive to traditional statistical measures. Such marriage of nonlinear time series analysis methods with machine learning algorithms could prove useful in developing a robust precursor technology that is capable of self learning. Recently, there have been many such advancements where data driven methods were used to unravel the physics behind nonlinear systems^{29–31}.

A specific advantage in utilizing deep-learning algorithms is their ability to analyze new data not limited to that from specific systems for which it was designed for. Some of the recent studies have focused on such methodologies to develop precursors for oscillatory instabilities in fluid dynamic systems^{32–36}. In this study, we combine both tools from nonlinear dynamics (recurrence, complex networks) and deep learning (CNN) to devise precursor to the onset of oscillatory instability.

Convolutional neural network is a widely used deep-learning algorithm for classifying and recognizing patterns present in multidimensional data and thus has the ability to autonomously extract essential patterns from an RN. In this study, we will utilize CNN to first classify recurrence networks corresponding to short time series segments of system variables to aperiodic and periodic segments. This classification is then used to quantify the state of intermittency by ascertaining the relative dominance of periodic and aperiodic dynamics of the system. Based on this information, we define a measure that indicates the proximity of the system to full-blown oscillatory instability. This measure can thus serve as a precursor for onset of oscillatory instability. We validate our prediction scheme by detecting the onset of oscillatory instability in a thermoacoustic system, aeroacoustic system and an aeroelastic system. The rest of the paper is organized in the following manner. First, in Sec. II, we describe the experimental system whose dynamics will be analyzed. In Sec. III, we discuss recurrence networks analysis and subsequently, in Sec. IV, we present the design of the convolutional neural networks and its implimentation to the problem in hand. In Sec. V, we share the results and assess the performance of the designed CNN in identifying the precursors to the instability. Finally, we end the exposition by discussing the future prospects in Sec. VI.

II. EXPERIMENTS

In this paper we will use experimental data from aeroacoustic, thermoacoustic and aeroelastic systems. By varying the respective control parameters in each of these systems, we observe the transition to the state of oscillatory instabilities. Schematics of the experimental setups are shown in Fig. 1. We provide a brief description of the experiments here.

The thermoacoustic system (Fig. 1a) consists of a settling chamber, a burner, combustion chamber, a bluff body as a flame stabilizing device, and a decoupler. Air enters through

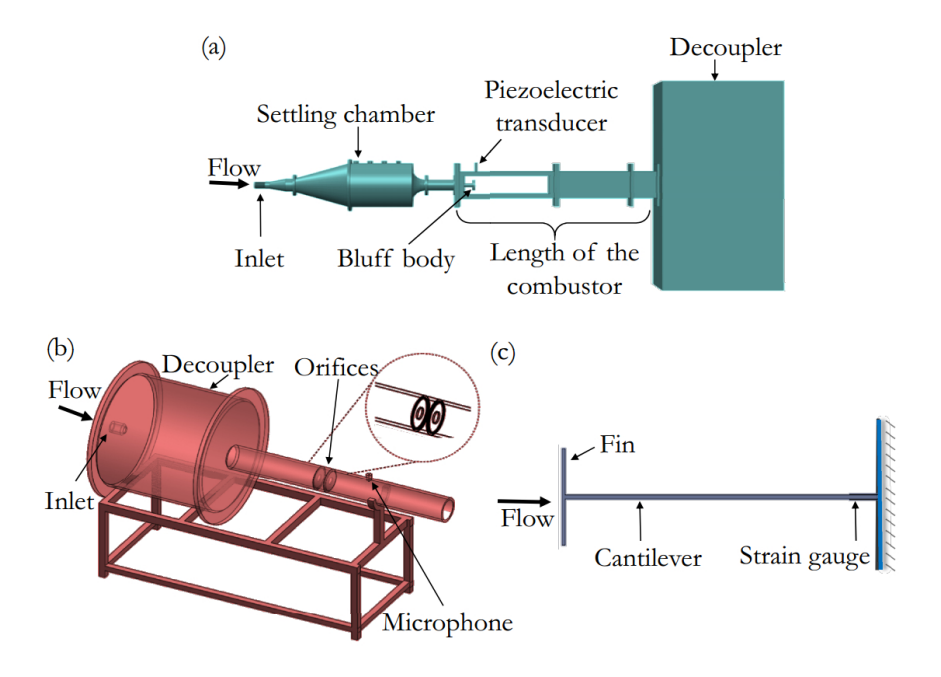


FIG. 1. a) Thermoacoustic system: A turbulent combustor with a bluff body stabilized flame b) Aeroacoustic system: Flow through orifice creating a tonal sound. c) Aeroelastic system: Flow over a finned cantilever. Reproduced with permission from EPL (Euro-physics Letters) 129, 24004 (2020)¹⁸. Copyright 2020, Institute of Physics

the inlet and it is partially premixed with the fuel (Liquid petroleum gas composed of propane-butane, mixed in 2:3 volume ratio). The combustion was initiated with spark generated in the combustor using a spark plug. In experiments, we vary the mass flow rate of air, keeping the mass flow rate of fuel constant thereby increasing the Re. Using a piezoelectric transducer (model: PCB103B02), we acquire unsteady pressure fluctuations for different values of Re as we increase it. The combustion dynamics transitions from a state of stable operation to thermoacoustic instability as Re is increased. Re is varied from 10,398 to 20,378. Further details including the uncertainties in the measurements for the corresponding experimental setup can be found in Raghunathan $et\ al.^{37}$.

An aeroacoustic system (shown in Fig. 1b) comprises a decoupler (the cylindrical chamber) and two orifices of diameter 20 mm located in a long duct (525 mm) with a spacing of 18 mm. An air flow is established through inlet and vortices are shed as it passes through the orifices. The feedback established between the vortex shedding and the acoustic field in the confinement results in the transition to aeroacoustic instability. We vary Re from 5615 \pm 185 to 9270 \pm 212 to observe this transition. Pressure fluctuations inside the duct are

measured using a pressure field pre-polarized microphone (model: 378C10) near 100 mm from the orifice. Details of this setup can be found in 18.

The third system where we study the transition is an aeroelastic system (Fig. 1c), which consists of a cantilever beam having length 45 mm (width = 25 mm & thickness = 0.5 mm). One side of the beam is fixed, and the other side is free. A small vertical fin (length = 12 mm) is attached to the free end of the cantilever. Air flow passes along the the length of the cantilever from left to right. The cantilever starts to oscillate due to the unsteady aerodynamic load created when there is vortex shedding from the fins. The resultant strain (S) is measured using a strain gauge, for different Re. We vary Re from 2384 \pm 159 to 4768 \pm 111 to capture the transition to aeroelastic instability. More details of this setup can be found in 18 .

III. CONSTRUCTION OF RECURRENCE NETWORKS

Recurrence is a fundamental property of a dynamical system due to which the system revisits the same part of the phase space repeatedly. The first step in performing recurrence analysis of a system is the reconstruction of the corresponding phase space trajectory, \vec{X} . We use Takens' embedding theorem to reconstruct the phase space, which allows one to reconstruct the phase space of a system using the time series of a state variable $x(t_i)$, where t_i represents the i^{th} time instant³⁸. By identifying an appropriate embedding dimension, d, and an optimal time lag, τ , we construct the dynamics along the d dimensions of the phase space as d time-delayed vectors derived from $x(t_i)$. If the length of $x(t_i)$ is x_i , the x_i element of x_i , x_i , is represented as:

$$\vec{X}_i = [x(t_i), x(t_i + \tau), \dots, x(t_i + (d-1)\tau)],$$

where $i = 1, \dots, N - \tau(d-1)$ (1)

Theoretically, any τ can be selected to reconstruct the phase space. Selecting a very small τ , will result in a phase space where it is not possible to distinguish the dynamics along two different neighboring dimensions. Whereas, by selecting a large τ , the dynamics along different dimensions become independent. We can identify an optimal τ to reconstruct the phase space such that the average mutual information between $x(t_i)$ and $x(t_i + \tau)$ is minimum³⁹. Additionally, an appropriate number of dimensions d, is chosen such that the

reconstructed phase space attractor appropriately unravels the phase space of the system, ensuring that the state points have a minimum number of false neighbors. Two neighboring points in a d-dimensional phase space are considered false neighbors if they do not remain neighbors in a reconstructed phase space with higher dimensions³⁹. A powerful method for finding optimal d, is an optimized version of Abarbanel's False Nearest Neighbors method, adapted by Cao⁴⁰. Here, we note that the focus of this work, is not on optimal reconstruction of the phase space. We rather aim to study how well CNN can classify recurrence networks, even when they are derived from a non-optimal reconstruction of the phase space. Hence, we select τ to be roughly equal to quarter of the time period of the periodic oscillations during oscillatory instability. d is chosen to be 6 since previous studies²⁸ show that for the low amplitude aperiodic oscillations, an embedding dimension of 6 is sufficient and for all other states, the embedding dimension is less than that. We define an unthresholded recurrence matrix R whose elements $R_{i,j}$ is given as:

$$R_{i,j} = \|\vec{X}_i - \vec{X}_j\|, \text{ where } i, j = 1, ..., N - \tau(d-1).$$
 (2)

We, then, proceed to derive a recurrence network from this recurrence matrix. A recurrence network is represented using an adjacency matrix A, whose elements are defined as:

$$A_{i,j} = \frac{1}{1 + R_{i,j}} - \delta_{i,j} \tag{3}$$

This definition ensures that, two nodes of the network, indicating state points at two instants of time, have a stronger bond (i.e. more weight) if they are closer in the phase space. The farther the nodes are in the phase space, the smaller the weight associated with the edge connecting them. Subtraction of Kronecker delta, $\delta_{i,j}$ in Eq. 3, ensures that the nodes of the network are not self-connected.

The network thus constructed from time series of a state variable can be visualized using the tool Gephi⁴¹ as shown in Fig. 2. Figure 2 represents recurrence networks corresponding to three dynamical states of a turbulent combustor i) low amplitude aperiodic oscillations known as combustion noise, ii) intermittency consisting of bursts of high amplitude periodic oscillations amidst low amplitude aperiodic oscillations and iii) thermoacoustic instability

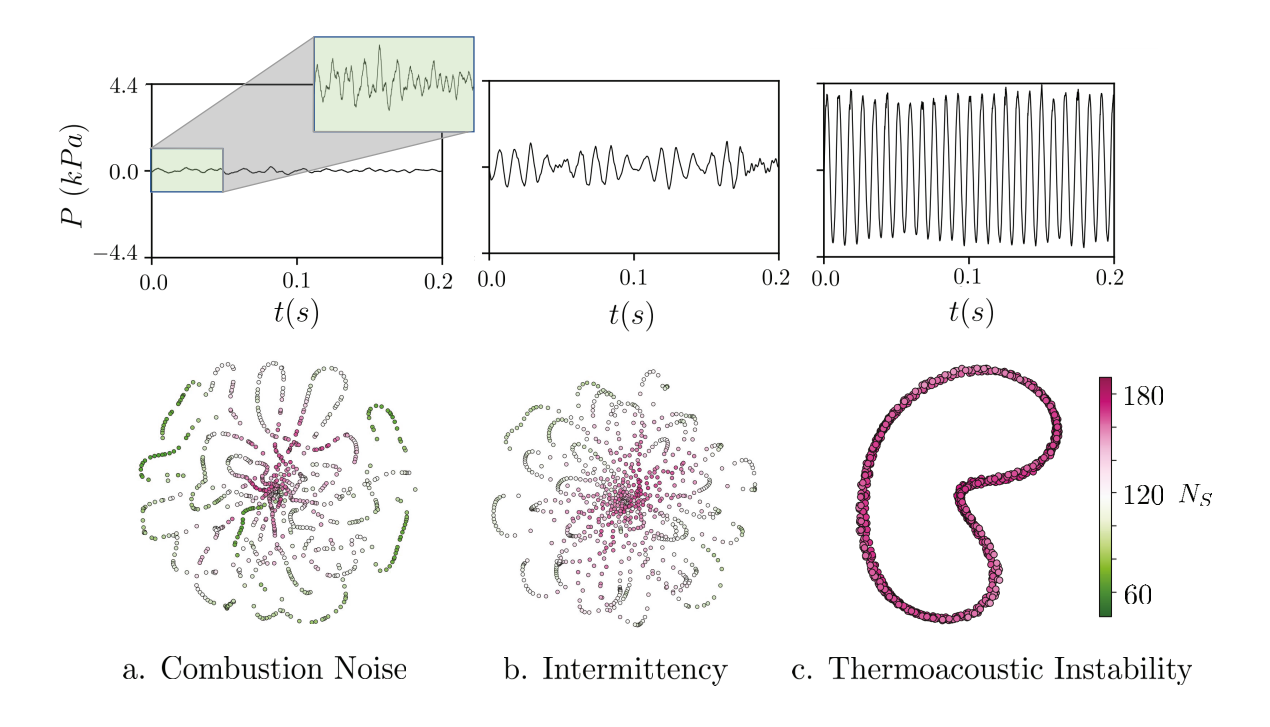


FIG. 2. Recurrence networks corresponding to three dynamical states in a thermoacoustic system a) aperiodic oscillations known as combustion noise with Re of 10398, b) intermittency with Re of 13230, c) oscillatory instability known as thermoacoustic instability with Re of 20,378. The node strength, N_S , is the sum of weights of all edges connected to a particular node.

characterized by high amplitude periodic oscillations. As mentioned before, such transitions occur as the Re of the flow is increased. These networks are constructed from the time series of unsteady pressure fluctuations. Recurrence networks preserve the geometry of the phase space attractor. Hence the recurrence network for aperiodic oscillations in a thermoacoustic system has a disorganized pattern with a widely varying node strength (N_S) . For periodic thermoacoustic oscillations, the corresponding network has a closed curve topology with a uniformly distributed N_S with a relatively higher value. During intermittency, we can observe a mixed nature for the network, where we see an increased N_S for some of the nodes and there are emerging closed curves in the network topology.

Once the recurrence networks are constructed as mentioned before, we use convolutional neural networks to extract salient features in the topology of those networks. This process is detailed in the following section.

IV. CONVOLUTIONAL NEURAL NETWORK

Inspired from the workings principle of a feline visual cortex, Convolutional Neural Networks (CNN) have become a popular type of Artificial Neural Network (ANN). An ANN consist of layers of interconnected artificial neurons resembling biological neural networks in a brain. This is achieved through a network of nodes across multiple layers, which are interconnected with links of non-uniform weights. These ANNs, then, form the foundation for deep learning. Given an input, the ANN has the ability to learn patterns from the input by accordingly adjusting the weights of the links that form the ANN. A CNN is a type of ANN in which some of the layers of the neural network also performs convolution on the input data⁴². First introduced for classification of handwritten characters⁴³, CNN possess many striking advantages. These networks have the ability to achieve shift invariance, i.e., the ability to identify the features in the input data regardless of their location. Furthermore, feature learning allows the network to extract only the important features from an input in order to make more accurate predictions. Lastly, weight sharing allows weights to be applied across an entire input, making this type of networks memory efficient^{44,45}.

The unique advantage of a CNN is centered on the convolutional layer, which is composed of multiple multidimensional weight matrices, referred to as filters. These filters perform convolution and thus, extract features in the input data (which, in our case is the adjacency matrix representing the complex network). For example, a diagonal filter \mathcal{F} shown in Fig. 3, when applied to the input adjacency matrix A, outputs the feature map B corresponding to the filter \mathcal{F} , following the rule:

$$B_{i,j} = \sum_{m=1}^{h} \sum_{n=1}^{w} A_{m-i,n-j} \mathcal{F}_{m,n}$$
(4)

Here, h and w are the height and width of the filter. For the particular case represented in Fig. 3, both h and w are equal to 3.

Once the feature maps are extracted the subsequent layers of the CNN processes the information in the feature maps for classification of the input data. Figure 4 represents a connection diagram for the entire CNN. First, the extracted feature maps are flattened into a one-dimensional array. The flattened array, is interconnected by weights, to a fully connected layer (FC), which is an array of nodes. FC identifies global patterns extracted by the convolutional layers and brings the information from all feature maps together to

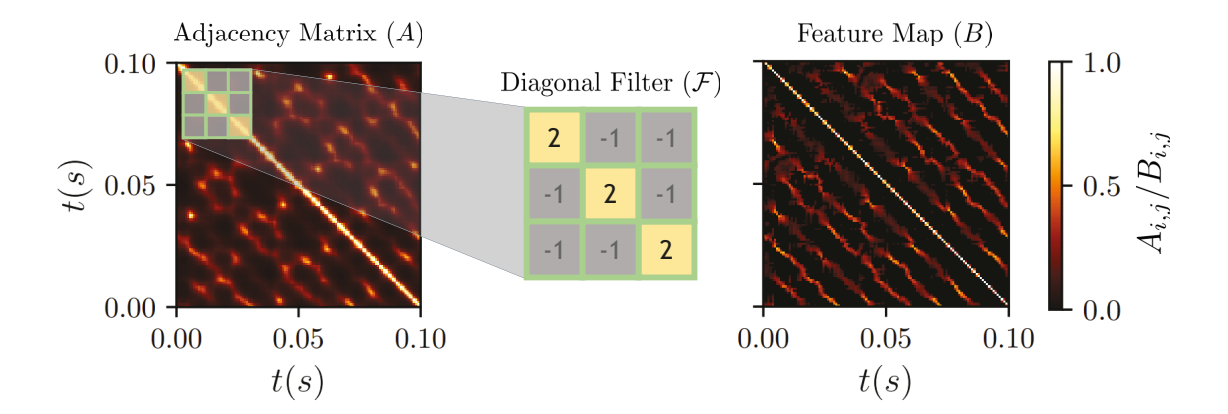


FIG. 3. Feature extraction using convolution layer. The Diagonal filter \mathcal{F} is convolved across the input adjacency matrix, A. The result of the convolution is the feature map, B, where the diagonal features from the input image are extracted.

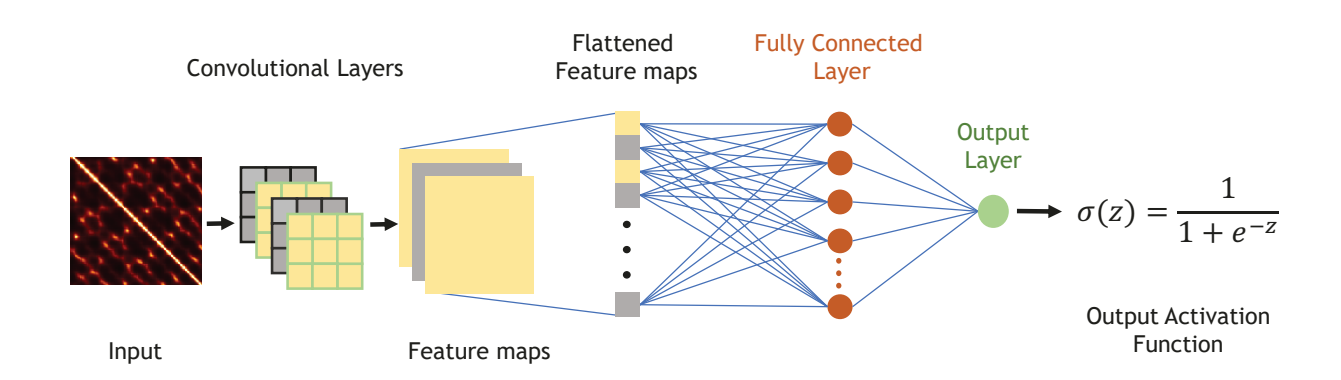


FIG. 4. The architecture of CNN designed to classify the structure of input recurrence network

perform classification.

We use a nonlinear activation function after each of these layers to equip CNN to extract complex features from the input data. An activation function, in essence, determines the response of an artificial neuron to stimuli. One of the most used activation function is Rectified Linear Unit (ReLU), which allows a relatively faster training process⁴⁶, and hence it is particularly advantageous over other nonlinear functions. Equation 5 shows that ReLU

function simply maps the negative inputs to zero and preserves the positive and zero inputs.

$$ReLU(B_{m,n}) = \begin{cases} B_{m,n} & \text{if } B_{m,n} > 0\\ 0 & \text{otherwise} \end{cases}$$
 (5)

Further, in order to increase the efficiency, the number operation needed by CNN is reduced by reducing the size of different layers through downsampling. Here, we utilize an effective form of commonly used downsampling method known as max pooling, where a window is slid over an input layer, and while the highest value in the window is selected to construct the next layer⁴⁷.

Typically the window will not overlap itself as it slides, it will only visit a set of data once. The result of this process is a compact version of the input layer.

Once the input data goes through the convolution layers and fully connected layers, the final step for classification is assigning a measure for each class that we are interested in identifying. In general, for the methodology we are describing, the different classes would be the different salient patterns in the phase space. In this study, we separate the input network into two class of salient patterns, i.e. periodic or aperiodic. Thus, we will utilize a sigmoid function as the classifier, which enables the intended binary classification. For more complex systems where higher number of classification is desired, a softmax function can be utilized⁴⁸. The sigmoid function outputs a value between zero and one, each corresponding to one of the two classes intended to be identified. During this process, the output of the FC layer is interconnected by weights to one node which makes up the output layer. The output of this node is, subsequently, fed into the sigmoid function as illustrated in Fig. 4.

A. Training the CNN

Inside the CNN, the process of learning simply entails adjusting the weight parameters of the network. By using already known information about the input, i.e., using a labelled data set, we can train the CNN. This mode of training using labelled data set is known as supervised learning. The objective of our CNN is to classify the input data (i.e., the Adjacency Matrix, A) into either periodic or aperiodic. The training data set thus contains labeled adjacency matrices. The label y of a binary classifier is either zero or one. In our case, one indicates that the input data is periodic and zero implies that the input data is aperiodic.

During the training process for classification using CNN, an input will pass through different layers of the CNN and provide some output (i.e., a number) indicative of different classes. In the initial phases of training, the untrained network is initialized with random weights and thus the output of classification will presumably be incorrect. Upon outputting an incorrect classification, the CNN computes a cost function which is a measure of the error between the value of y that CNN predicts (\hat{y}) and the value of y actually is (obtained from the known label). The cost function utilized in our CNN is a version of binary cross entropy⁴⁹, a typical cost function used for a binary classifier problem. Binary Cross entropy is expressed in Eq. 6, where \hat{y} is the output of the CNN for an input A with label y.

$$J = -y \ln \hat{y} + (1 - y) \ln (1 - \hat{y}) \tag{6}$$

In the case when the prediction of the CNN, \hat{y} , is equal to the known classifier label y. The value of the cost function, J is approximately zero. On the other hand, if the prediction value deviates from the known classifier value, then the cost function will tend to infinity.

After identifying the cost for a set of predictions for the training data. An average cost is estimated. Given this average cost, we perform a process known as error back propagation. That is, by going back through the different layers of the networks, we adjust the weights of CNN to minimize the average cost. This is done utilizing Adam optimization⁵⁰, a variation of gradient descent method. Multiple iterations of cost minimization through back propagation will make the output of CNN a more accurate representation of the known classification y. It is also noted that, through the process of supervised training, the weights in the filters also are adjusted to optimize the cost. Much like the example with the diagonal filter in Figure 3, the filters in the CNN will extract certain features. However, instead of hand-engineered filters, through back propagation in the CNN training process, the system identifies most essential filters for classifying the input. A more detailed introduction on the layers, functions, and back-propagation of a CNN is given in the monograph by Wu⁵¹. The complete structure of the CNN used in the present study is detailed in Table I.

TABLE I. Structure of the CNN

Name	Dimensions	Operations
Input Adjacency Matrix	122×122	None
Conv-1	$120\times120\times32$	$3\times3\times32$ Convolution
Activation-1	$120\times120\times32$	ReLU Activation
MaxPool-1	$60 \times 60 \times 32$	2x2 Max Pooling
Conv-2	$58 \times 58 \times 32$	$3\times3\times32$ Convolution
Activation-2	$58 \times 58 \times 32$	ReLU Activation
MaxPool-2	$29{\times}29{\times}32$	2x2 Max Pooling
Flatten	26912	Converting to one column vector
FC-1	64	64 Fully-Connected
Activation-3	64	ReLU Activation
FC-2	1	1 Fully-Connected
Activation-4	1	Sigmoid Activation

V. PRECURSOR MEASURE AND ITS IMPLEMENTATION AS AN EARLY WARNING FOR ONSET OF OSCILLATORY INSTABILITY

The CNN described in the previous sections is trained to distinguish aperiodic structures in the recurrence network from periodic patterns. The input time series segment for each classification has a length δL . We scan the input time series of length L in overlapping segments of length δL with an overlap of ΔL . Using Eq. 3, the corresponding adjacency matrix, A, for each time series segment is identified which then is passed through the trained CNN. We, subsequently, label each time series segment with the output classification of CNN, \hat{y} as its periodic probability value, μ_0 . The CNN is trained such that μ_0 is 1 if the dynamics is purely periodic and sinusoidal. As the dynamics moves closer to aperiodic, the probability value moves closer to 0. It is to be noted that depending on the system, the aperiodic fluctuations of the system variable could resemble white/colored noise or that of chaotic turbulent fluctuations exhibiting high short-time correlations. Since we train the CNN with all possible types of noise signals, the advantage of the present method is that it is able to identify and assign a value of μ_0 close to zero for all such types of 'noise' signals.

Figure 5 shows such labeling of local dynamics using CNN for a time series segment of a state variable measured from a thermoacoustic system (corresponding images for aeroacoustic and aeroelastic systems are given in the Appendix). The color of the background of the time series represent the local periodic probability value (μ_0).

We also define a precursor measure (μ) for the dynamic state represented by the time series of state variable to be the average of the probability measure, μ_0 calculated for all overlapping segments of length dL that constitute the time series segments of length L. In all cases considered in this manuscript, we consider L=3 s, $\delta L=0.03$ s and $\Delta L=0.02$ s. A good rule of thumb to follow is that L should be of the order of 100T (ensuring that intermittency statistics converge) and δL should be of the order of 3T (ensuring we at least cover 3 cycles of oscillation in each time series segments), where T is the time period of oscillations.

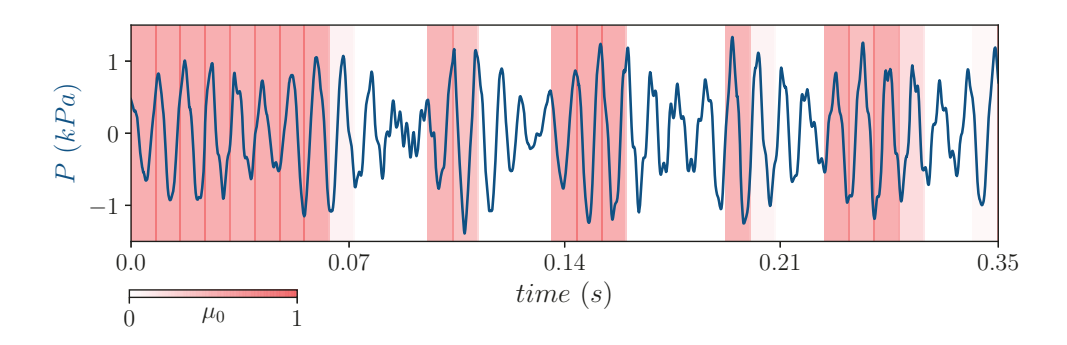


FIG. 5. Probability of periodicity (μ_0) measured for different parts of an intermittent pressure fluctuation taken from thermoacoustic experiments ($Re = 1.3 \times 10^4$). The background color represent μ_0 . $\mu_0 = 1$ if the oscillations are periodic and $\mu_0 = 0$ if oscillations are aperiodic. Here, parameters $\delta L = 0.03 \ s$ (window size) and $\Delta L = 0.02 \ s$ (overlap).

In Fig. 6, we show the variation of μ with the control parameter (Re) for all three systems. Here, the experiments were conducted in a quasi-steady manner, in that the control parameter was changed in steps and the data was obtained for each step ensuring that the control parameter remained steady for the duration of data acquisition. The time series of state variables for all systems illustrated in top rows of Fig. 6 are 3 s long, each for different control parameter values, and subsequently joined together one after the other for the purpose of illustration. The alternating white and gray backgrounds in the time series

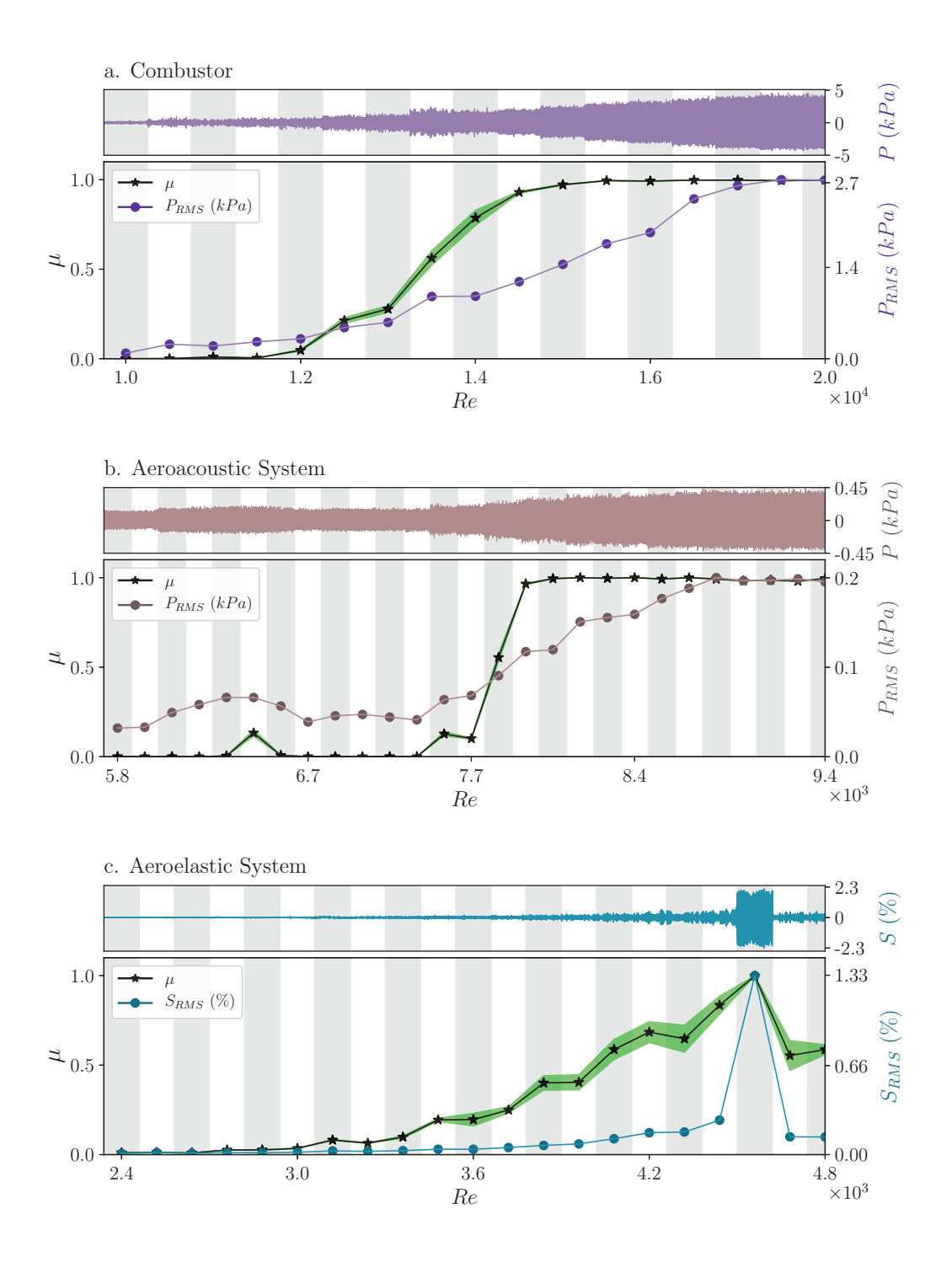


FIG. 6. Precursor for onset of oscillatory instability in fluid dynamic systems. a) Thermoacoustic system b) Aeroacoustic system c) Aeroelastic System. In all cases, the top panel show the fluctuations of system variable, measured for quasistatic variation of control parameter, Re.

indicate each 3 s long segment corresponding to a particular control parameter value.

In the bottom rows of Fig. 6 for three systems, we plot the RMS of the time segments and probability of periodicity μ , as identified by the CNN. We see that μ is able to detect the transition in all systems. Once μ is estimated, the operator can set appropriate thresholds for controlling the fluid systems. For the combustor, the onset of instability is detected much before P_{RMS} saturates to a high value. In the case of the aeroacoustic system, even though the P_{RMS} varies gradually as we approach acoustic instability, the variation in μ indicates that the transition to oscillatory instability is rather abrupt. In the case of aeroelastic system, the amplitude of strain oscillations abruptly increase upon the onset of oscillatory instability. However, we see that μ is able to detect an impending transition in the dynamics far away from the onset of oscillatory instability.

Note that as this warning system is repeatedly implemented on new data, it can also be retrained with the new data enabling self learning. In the present study, we discussed only the onset of single mode oscillatory instabilities. The methodology to analyze dynamical systems introduced here focusing on the combined use of dynamical systems theory and deep learning, can also be extended for classification of different dynamical states of a general dynamical system and bifurcation analysis.

VI. SUMMARY AND FUTURE PROSPECTS

We introduced a methodology to quantify the relative dominance of different salient topological features of a complex phase space attractor by analyzing patterns in the corresponding recurrence networks using convolutional neural networks. This methodology is particularly useful in classifying various dynamical states of practical systems. The relative dominance of salient features of phase space topology can be used as an identifier for the dynamical state of the system and a measure derived based on this information can be used both to analyze and identify the state of a practical system, and thus aid its control. This methodology can also provide early warning impending dynamical transitions in the system.

We implemented this methodology to devise a framework for early detection of the onset of oscillatory instability in fluid dynamic systems encompassing turbulent flows. The CNN was able to ascertain the relative dominance of periodic and aperiodic dynamics during the dynamical state of intermittency and thus estimate the proximity of the fluid dynamic system to full-blown oscillatory instability. We successfully implemented the early warning system for three fluid systems with significantly different characteristics, a thermoacoustic system, an aeroacoustic system and an aeroelastic system.

An advantage that network approaches provide in analyzing a dynamical system is their ability to incorporate either physical or abstract connections across layers of networks of information about the system, based on some chosen rules. Here, the different layers of networks could represent different subsystems of the system, different spatial locations of the system, different temporal regimes and so on. During the temporal evolution of dynamics, these interconnections get rewired. Studying this new representation of data in terms of networks can be very fruitful.

Traditional network measures mostly provide the averaged topological statistics of the network. However, tools from machine learning would be able to capture variations in complex patterns in networks. Thus the combination of network analysis and machine learning could enable us to investigate variation in inter subsystem dependencies, spatial flow of information, temporal correlations and causal relations in a dynamic system with much more flexibility and detail.

ACKNOWLEDGEMENTS

The research at the University of California, San Diego, was supported by internal grants from the Jacobs School of Engineering and US National Science Foundation (CBET, Grant 2053671).

DATA AVAILABILITY

The data that support the findings of this study are available upon request.

APPENDIX

The variation of μ_0 measured for time series segments obtained for aeroacoustic and aeroelastic experiments are given in Fig. 7 and Fig. 8, respectively.

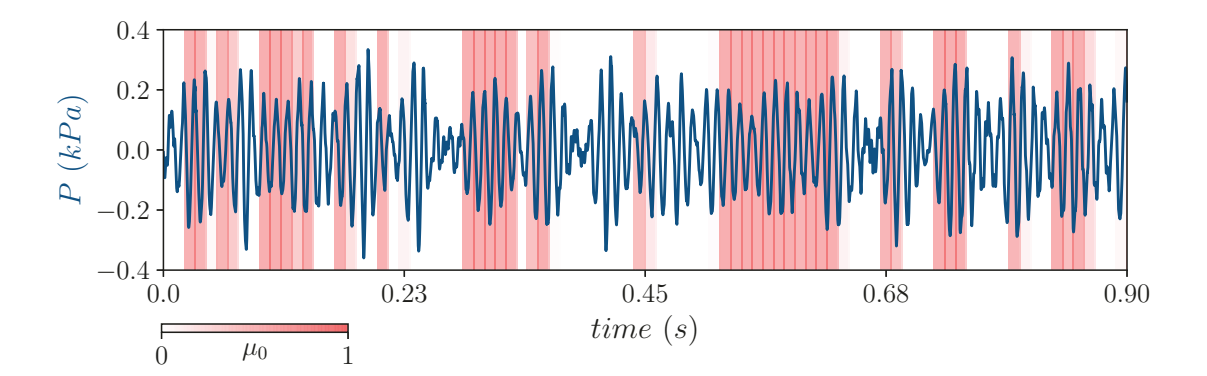


FIG. 7. Probability of periodicity (μ_0) measured for different parts of an intermittent pressure fluctuation taken from aeroacoustic experiments ($Re = 7.8 \times 10^3$). The background color represent μ_0 . $\mu_0 = 1$ if the oscillations are periodic and $\mu_0 = 0$ if oscillations are aperiodic.

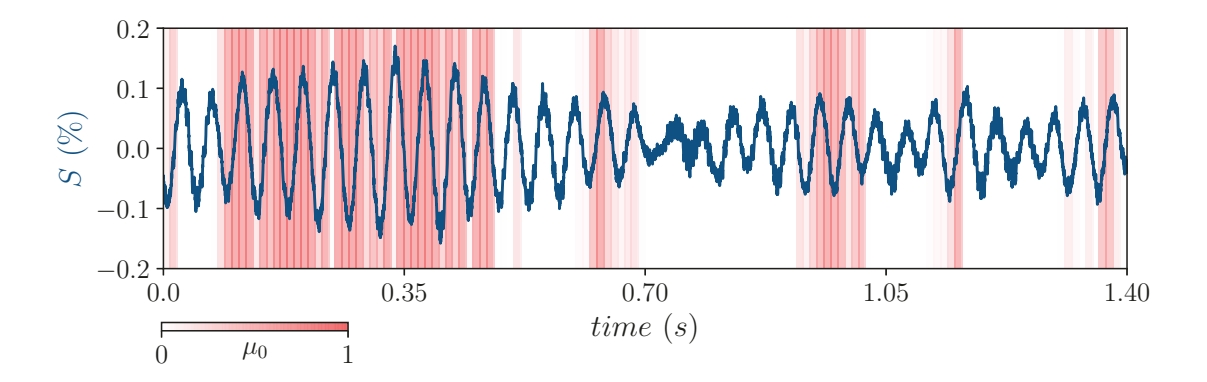


FIG. 8. Probability of periodicity (μ_0) measured for different parts of an intermittent strain fluctuation taken from aeroelastic experiments ($Re = 3.8 \times 10^3$). The background color represent μ_0 . $\mu_0 = 1$ if the oscillations are periodic and $\mu_0 = 0$ if oscillations are aperiodic.

REFERENCES

- 1 T. Poinsot, "Prediction and control of combustion instabilities in real engines," Proceedings of the Combustion Institute **36**, 1 28 (2017).
- ²T. C. Lieuwen, *Unsteady combustor physics* (Cambridge University Press, 2012).
- ³A. P. Dowling and J. E. Ffowcs Williams, Sound and sources of sound (Horwood, 1983).
- ⁴D. Rockwell and E. Naudascher, "Self-sustained oscillations of impinging free shear layers," Annual Review of Fluid Mechanics **11**, 67–94 (1979).

- ⁵J. Panda, "An experimental investigation of screech noise generation," Journal of Fluid Mechanics **378**, 71–96 (1999).
- ⁶D. Middleton, "Theoretical and experimental investigations into the acoustic output from ejector flows," Journal of Sound and Vibration **11**, 447–473 (1970).
- ⁷G. A. Flandro and J. Majdalani, "Aeroacoustic instability in rockets," AIAA Journal **41**, 485–497 (2003).
- ⁸K. A. Kurbatskii and R. R. Mankbadi, "Review of computational aeroacoustics algorithms," International Journal of Computational Fluid Dynamics **18**, 533–546 (2004).
- ⁹J. F. Williams, "Aeroacoustics," Annual Review of Fluid Mechanics **9**, 447–468 (1977).
- ¹⁰A. Larsen, "Aerodynamics of the tacoma narrows bridge-60 years later," Structural Engineering International **10**, 243–248 (2000).
- ¹¹M. H. Hansen, "Aeroelastic instability problems for wind turbines," Wind Energy: An International Journal for Progress and Applications in Wind Power Conversion Technology **10**, 551–577 (2007).
- ¹²G. A. Richards, D. L. Straub, and E. H. Robey, "Passive control of combustion dynamics in stationary gas turbines," Journal of Propulsion and Power 19, 795–810 (2003).
- ¹³J. Lee and D. Santavicca, "Experimental diagnostics for the study of combustion instabilities in lean premixed combustors," Journal of propulsion and power **19**, 735–750 (2003).
- ¹⁴B. Korbahti, E. Kagambage, T. Andrianne, N. A. Razak, and G. Dimitriadis, "Subcritical, nontypical and period-doubling bifurcations of a delta wing in a low speed wind tunnel," Journal of Fluids and Structures 27, 408–426 (2011).
- ¹⁵V. Nair, G. Thampi, and R. I. Sujith, "Intermittency route to thermoacoustic instability in turbulent combustors," Journal of Fluid Mechanics **756**, 470–487 (2014).
- ¹⁶V. Nair and R. I. Sujith, "Precursors to self-sustained oscillations in aeroacoustic systems," International Journal of Aeroacoustics **15**, 312–323 (2016).
- ¹⁷J. Venkatramani, V. Nair, R. I. Sujith, S. Gupta, and S. Sarkar, "Precursors to flutter instability by an intermittency route: a model free approach," Journal of Fluids and Structures **61**, 376–391 (2016).
- ¹⁸I. Pavithran, V. R. Unni, A. J. Varghese, R. I. Sujith, A. Saha, N. Marwan, and J. Kurths, "Universality in the emergence of oscillatory instabilities in turbulent flows," EPL (Europhysics Letters) **129**, 24004 (2020).

- ¹⁹I. Pavithran, V. R. Unni, A. J. Varghese, D. Premraj, R. I. Sujith, C. Vijayan, A. Saha, N. Marwan, and J. Kurths, "Universality in spectral condensation," Scientific Reports 10, 1–8 (2020).
- ²⁰R. I. Sujith and V. R. Unni, "Complex system approach to investigate and mitigate thermoacoustic instability in turbulent combustors," Physics of Fluids **32**, 061401 (2020).
- ²¹V. Nair, G. Thampi, and R. I. Sujith, "Intermittency route to thermoacoustic instability in turbulent combustors," Journal of Fluid Mechanics **756**, 470–487 (2014).
- ²²V. Nair and R. I. Sujith, "Multifractality in combustion noise: predicting an impending combustion instability," Journal of Fluid Mechanics **747**, 635–655 (2014).
- ²³V. R. Unni, A. Mukhopadhyay, and R. I. Sujith, "Online detection of impending instability in a combustion system using tools from symbolic time series analysis," International Journal of Spray and Combustion Dynamics 7, 243–255 (2015).
- ²⁴H. Gotoda, Y. Shinoda, M. Kobayashi, Y. Okuno, and S. Tachibana, "Detection and control of combustion instability based on the concept of dynamical system theory," Phys. Rev. E 89, 022910 (2014).
- ²⁵M. Murugesan and R. I. Sujith, "Combustion noise is scale-free: transition from scale-free to order at the onset of thermoacoustic instability," Journal of Fluid Mechanics **772**, 225 (2015).
- ²⁶V. Godavarthi, V. R. Unni, E. A. Gopalakrishnan, and R. I. Sujith, "Recurrence networks to study dynamical transitions in a turbulent combustor," Chaos: An Interdisciplinary Journal of Nonlinear Science **27**, 063113 (2017).
- ²⁷V. Nair, G. Thampi, and R. I. Sujith, "Engineering precursors to forewarn the onset of an impending combustion instability," in *Turbo Expo: Power for Land, Sea, and Air*, Vol. 45691 (American Society of Mechanical Engineers, 2014) p. V04BT04A005.
- ²⁸V. Godavarthi, S. A. Pawar, V. R. Unni, R. I. Sujith, N. Marwan, and J. Kurths, "Coupled interaction between unsteady flame dynamics and acoustic field in a turbulent combustor," Chaos: An Interdisciplinary Journal of Nonlinear Science 28, 113111 (2018).
- ²⁹M. Quade, T. Isele, and M. Abel, "Machine learning control—explainable and analyzable methods," Physica D: Nonlinear Phenomena **412**, 132582 (2020).
- ³⁰M. Schmidt and H. Lipson, "Distilling free-form natural laws from experimental data," science **324**, 81–85 (2009).

- ³¹H. U. Voss, P. Kolodner, M. Abel, and J. Kurths, "Amplitude equations from spatiotemporal binary-fluid convection data," Physical review letters **83**, 3422 (1999).
- ³²U. Sengupta, G. Waxenegger-Wilfing, J. Martin, J. Hardi, and M. Juniper, "Avoiding high-frequency thermoacoustic instabilities in liquid propellant rocket engines using bayesian deep learning," Bulletin of the American Physical Society (2020).
- ³³T. Hachijo, H. Gotoda, T. Nishizawa, and J. Kazawa, "Experimental study on early detection of cascade flutter in turbo jet fans using combined methodology of symbolic dynamics, dynamical systems theory, and machine learning," Journal of Applied Physics 127, 234901 (2020).
- ³⁴T. Kobayashi, S. Murayama, T. Hachijo, and H. Gotoda, "Early detection of thermoacoustic combustion instability using a methodology combining complex networks and machine learning," Physical Review Applied 11, 064034 (2019).
- ³⁵C. Bhattacharya, J. O'Connor, and A. Ray, "Data-driven detection and early prediction of thermoacoustic instability in a multi-nozzle combustor," Combustion Science and Technology, 1–32 (2020).
- ³⁶S. Mondal, N. F. Ghalyan, A. Ray, and A. Mukhopadhyay, "Early detection of thermoacoustic instabilities using hidden markov models," Combustion Science and Technology (2018).
- ³⁷M. Raghunathan, N. B. George, V. R. Unni, P. R. Midhun, K. V. Reeja, and R. I. Sujith, "Multifractal analysis of flame dynamics during transition to thermoacoustic instability in a turbulent combustor," Journal of Fluid Mechanics 888, A14 (2020).
- ³⁸S. H. Strogatz, Nonlinear dynamics and chaos with student solutions manual: With applications to physics, biology, chemistry, and engineering (CRC press, 2018).
- ³⁹H. D. I. Abarbanel, R. Brown, J. J. Sidorowich, and L. S. Tsimring, "The analysis of observed chaotic data in physical systems," Rev. Mod. Phys. **65**, 1331–1392 (1993).
- ⁴⁰L. Cao, "Practical method for determining the minimum embedding dimension of a scalar time series," Physica D: Nonlinear Phenomena **110**, 43 50 (1997).
- ⁴¹M. Bastian, S. Heymann, and M. Jacomy, "Gephi: An open source software for exploring and manipulating networks," (2009).
- ⁴²K. O'Shea and R. Nash, "An introduction to convolutional neural networks," (2015), arXiv:1511.08458 [cs.NE].

- ⁴³Y. Lecun, L. Bottou, Y. Bengio, and P. Haffner, "Gradient-based learning applied to document recognition," Proceedings of the IEEE **86**, 2278 2324 (1998).
- ⁴⁴T. Liu, S. Fang, Y. Zhao, P. Wang, and J. Zhang, "Implementation of training convolutional neural networks," (2015), arXiv:1506.01195 [cs.CV].
- ⁴⁵S. L. Brunton, B. R. Noack, and P. Koumoutsakos, "Machine learning for fluid mechanics," Annual Review of Fluid Mechanics **52**, 477–508 (2020).
- ⁴⁶A. Krizhevsky, I. Sutskever, and G. E. Hinton, "Imagenet classification with deep convolutional neural networks," in *Advances in Neural Information Processing Systems 25*, edited by F. Pereira, C. J. C. Burges, L. Bottou, and K. Q. Weinberger (Curran Associates, Inc., 2012) pp. 1097–1105.
- ⁴⁷D. Scherer, A. Müller, and S. Behnke, "Evaluation of pooling operations in convolutional architectures for object recognition," in *International conference on artificial neural networks* (Springer, 2010) pp. 92–101.
- ⁴⁸A. Krizhevsky, I. Sutskever, and G. E. Hinton, "Imagenet classification with deep convolutional neural networks," Advances in neural information processing systems **25**, 1097–1105 (2012).
- ⁴⁹P.-T. De Boer, D. P. Kroese, S. Mannor, and R. Y. Rubinstein, "A tutorial on the cross-entropy method," Annals of operations research **134**, 19–67 (2005).
- ⁵⁰D. P. Kingma and J. Ba, "Adam: A method for stochastic optimization," (2017), arXiv:1412.6980 [cs.LG].
- ⁵¹J. Wu, "Introduction to convolutional neural networks," National Key Lab for Novel Software Technology. Nanjing University. China **5**, 23 (2017).